Journal of Neuroscience Methods 130 (2003) 143–157

JOURNAL OF NEUROSCIENCE METHODS

www.elsevier.com/locate/jneumeth

Combining deconvolution and fluctuation analysis to determine quantal parameters and release rates

Erwin Neher*, Takeshi Sakaba

Department of Membrane Biophysics, Max Planck Institute for Biophysical Chemistry, Am Fassberg 11, 37077 Göttingen, Germany

Accepted 8 September 2003

Abstract

Analysis methods are described which integrate information from fluctuation analysis with that from deconvolution. Together the two approaches allow to derive a consistent quantitative description of quantal release (both evoked, spontaneous and asynchronous) under conditions in which quantal parameters may change during a repetitively applied stimulation protocol. Specifically, our methods take into account the effects of accumulating transmitter in the synaptic cleft and postsynaptic receptor desensitization, which may develop during strong stimulation. Several ways to handle non-stationarities are described. Examples are provided for the Calyx of Held, a glutamatergic synapse, in which both the pre- and the postsynaptic compartments can be voltage-clamped.
© 2003 Elsevier B.V. All rights reserved.

Keywords: Synapse; Vesicle; Transmitter; Calyx of Held; Glutamate; Quantal analysis; Synaptic modulation; Cumulants

1. Introduction

Synaptic transmission is a highly probabilistic process. Stochastic events occur on at least two levels of resolution: first, the release of quanta of transmitter (Katz, 1969), which typically activate tens or hundreds of channels each and second, the opening and closing of individual channels (Anderson and Stevens, 1973; Katz and Miledi, 1972). Under many circumstances the resulting stochastic fluctuations in postsynaptic signals are just noise, which the researcher wants to minimize. However, early-on it was recognized that this noise carries information on the molecular events underlying the signals (Anderson and Stevens, 1973; Katz and Miledi, 1972) and methods which extract this information were developed (for overview, see Colquhoun and Hawkes, 1981; Fesce, 1990; Neher and Stevens, 1977). The theories underlying such techniques usually make idealizing assumptions about the stochastic processes involved, such as stationarity of continuous current records or stationarity in ensemble records in the sense that starting conditions for all records of an ensemble are identical. Many such identical traces or long stretches of stationary record are desirable for good signal to noise ratio of the estimates. Unfortunately, most synapses and molecules involved, however, do not conform: channels desensitize or inactivate on several time scales, and synapses facilitate or depress. Rarely is it possible to obtain tens or even hundreds of stationary records for ensemble analysis, because the preparation 'runs down' and access resistance starts to deteriorate. Moreover, fluctuations from various sources, such as channel noise and quantal noise, often overlap. Fortunately, however, conditions at glutamatergic synapses are such that simple manipulations mitigate or even effectively eliminate the adverse effects of such uncooperative behavior. This review tries to summarize recent experiences, mainly from our laboratory, in adapting noise analysis techniques to the specific circumstances of a glutamatergic synapse. We also show how information from noise analysis can be combined with the technique of deconvolution to overcome a serious obstacle in the application of this technique to synapses in brain slices, namely accumulation of transmitter in the synaptic cleft and concomitant cross-talk between neighboring release sites (Barbour and Häusser, 1997). Although most of the results mentioned in this review derive from experiments at the Calyx of Held—a giant glutamatergic terminal, which allows simultaneous voltage clamping of pre- and postsynaptic compartments—the analysis can also readily be applied to other synapses, as will be discussed below. We will start

* Corresponding author. Tel.: +49-551-201-1630; fax: +49-551-201-1688.
E-mail address: eneher@gwdg.de (E. Neher).

0165-0270/$ – see front matter © 2003 Elsevier B.V. All rights reserved.
doi:10.1016/j.jneumeth.2003.09.020

with noise analysis, because an understanding of some aspects of this technique is necessary for its combination with deconvolution.

2. Noise analysis on the basis of Campbell's theorem

In synaptic physiology we are very often confronted with records that consist of random superpositions of miniature currents or miniature potentials. These may occur spontaneously, as a consequence of manipulations which elevate intracellular [Ca^{2+}], or due to asynchronous release after intense stimulation. At the Calyx of Held, which allows controlled presynaptic depolarization, miniature excitatory postsynaptic currents (mEPSCs) can be elicited within a wide range of release rates. Campell's theorem, which is an outflow of the electronics communication technology of early last century (Rice, 1944), is ideally suited to handle such signals. The theorem considers streams of stochastically occurring elementary signals (such as noise spikes on a telephone line), which occur statistically independently at a certain mean rate and superimpose linearly. If such elementary events are relatively brief compared to the total observation interval T, and if the rate of occurrence ξ, is stationary within this interval, then the theorem states (in its simplest form!) that both the mean signal and the variance of the signal should be proportional to this rate. The proportionality constant between mean and rate is the area under the elementary signal and the relevant constant for the variance is the area under the square of the elementary signal. Furthermore, the same approach can be extended to the higher moments of the signal (i.e. the normalized integral over the nth power of the signal) such as skewness (third power) and kurtosis (fourth power). In all cases so-called 'cumulants', which are combinations of moments up to the given power, have to be considered (see below and Appendix A).

Segal et al. (1985) and Fesce et al. (1986) perfected this approach for studies at the neuromuscular junction. They considered elementary signals of peak amplitude h, with normalized time course $F(t)$ occurring at rate ξ. With this notation an mEPSC, occurring at time t' has the time course $hF(t-t')$ and Campbell's theorem can be written as

$$\lambda_n = \xi h^n \int [F(t)]^n \, \mathrm{d}t \equiv \xi h^n I_n \tag{1}$$

Here, λ_n is the nth cumulant, the integration extends over the whole time during which $F(t)$ is non-zero and I_n was introduced as a short-hand notation for $\int [F(t)]^n \, \mathrm{d}t$. The application of Campell's theorem to the cases $n = 2$ (variance) and $n = 1$ (mean) results in $\lambda_2/\lambda_1 = hI_2/I_1$, which is the well-known result that the elementary signal amplitude is proportional to the ratio of variance and mean. In fact, for single channel responses (elementary signals are square pulses with $I_2/I_1 = 1$) the single channel amplitude is just the ratio of λ_2 and λ_1. For instantaneously rising and exponentially decaying signals (such as 'ideal' mEPSCs), the ratio $I_2/I_1 = 1/2$ as already pointed out by Katz and Miledi (1972). Likewise, the ratios $I_\nu/I_{\nu-1}$ can be evaluated for any given shape of the elementary signal and, in principle, any ratio between successive cumulants can be used to determine h.

In the analysis described so far, many simplifying assumptions were made: background noise was neglected, ideal stationarity was assumed, and the 'elementary signal' was assumed to have a well-determined time course (as may be appropriate for noise spikes in electronic circuits). Particularly, the last assumption is usually invalid for biological signals, since we know, for instance, that single channel signals are not identical to each other. They have a characteristic distribution of open times and, likewise, most mEPSCs have some dispersion in their amplitudes. These aspects, however, are readily accommodated, if one can assume that the elementary events, indeed, are statistically independent among themselves and also are independent of the signals which generate background noise. In this case, the basic laws regarding the linear superposition of random variables state that for such signals the cumulants add linearly (see Appendix A). This is trivial for the mean values but it also holds for the variance in the following sense: if a random signal, y, is the sum of two independent signals y_1 and y_2, then the variance σ_y^2 of y is the sum of the variances $\sigma_{y_1}^2$ and $\sigma_{y_2}^2$. Applying this law tells us that we can subtract the variance of the background noise from the measured total noise in order to obtain the variance of the mEPSCs and, in addition, we can (mentally!) subdivide all single channel events into subclasses of certain durations, and apply Campbell's theorem for each class individually. In the case of single channel responses this is particularly simple because for each subclass the same result is obtained ($h = \lambda_2/\lambda_1$; $I_2/I_1 = 1$), such that the overall result is again the simple ratio λ_2/λ_1. In the case of mEPSCs with a size distribution, $g(h)$, of amplitudes and the same shape factors (I_n) for the different sizes the situation is somewhat more complicated:

$$\lambda_2 = \sigma_y^2 = \xi \int I_2 h^2 g(h) \, \mathrm{d}h = \xi \langle h^2 \rangle I_2 \tag{2}$$

$$\lambda_1 = \langle y \rangle = \xi \int I_1 h g(h) \, \mathrm{d}h = \xi \langle h \rangle I_1 \tag{3}$$

such that

$$\frac{\lambda_2}{\lambda_1} = \langle h \rangle \frac{\langle h^2 \rangle}{\langle h \rangle^2} \frac{I_2}{I_1} \tag{4}$$

Here, $\langle y \rangle$ and $\langle h \rangle$ denote the expectation value of y and h, respectively, and the equation was written in a form, which subdivides the result into that obtained for a uniform or narrow amplitude distribution ($\lambda_2/\lambda_1 = \langle h \rangle I_2/I_1$) and a 'correction factor', $\langle h^2 \rangle / \langle h \rangle^2$, which reflects the relative width of the amplitude distribution. For a Gaussian with mean

$\bar{h}$ and width σ_n this correction factor is $(1 + (\sigma_n^2/\langle h\rangle^2))$. It should also be noted that the assumption of 'statistical independence' of elementary events implies a low degree of activation of the physiological processes involved. Thus, for the case of ion channel signals we imply low open probability p. In the case of release of quanta from presynaptic terminals, we imply the limit of Poisson statistics (because for a large degree of activation, requiring Binomial statistics, the probability of release of a quantum depends on how many quanta are still available for release or how many quanta have already been released).

3. Separating channel noise from quantal noise: employing higher moments or predicting channel variance from mean current

When mEPSCs summed, they may build up to a substantial average current, which fluctuates strongly due to the random arrival of new events. However, part of these fluctuations also come from random open–close fluctuations of channels during the decaying phases of previous mEPSCs (Faber et al., 1992). Also, transmitter may build up in the synaptic cleft and elicit so-called 'residual current' (Barbour et al., 1994; Carter and Regehr, 2000; Faber and Korn, 1988; Hartzell et al., 1975; Kinney et al., 1997; Otis et al., 1996; Trussell et al., 1993) by activating postsynaptic channels. Thus, total variance measured in the postsynaptic record has three sources: background variance $\lambda_{2,o}$, ion channel variance $\lambda_{2,c}$ and the variance of interest, $\lambda_{2,q}$ (q for quantal noise). $\lambda_{2,o}$ in most cases can be measured as the variance before or after activation of mEPSCs or as the y-axis intercept in a plot of total variance against mean current, I_p (if stretches of record with different degrees of synaptic activation are available). Channel variance $\lambda_{2,c}$ in most cases of interest is the product of a mean single channel amplitude i and mean postsynaptic current I_p, such that (assuming all three sources of noise can be considered statistically independent) we can write

$$\lambda_2 = \lambda_{2,o} + iI_p + \lambda_{2,q} \tag{5}$$

A critical question is: can we assume statistical independence of channel variance and quantal variance? This is not trivial, since, of course, quanta are made up of fluctuating ion channels. The answer, however, is that it is safe to do so in most cases of interest. Arguments in favor of this assertion are given by Neher and Sakaba (2001b), where the assumption was also tested by numerous Monte Carlo simulations. Thus, with Eq. (5) we can calculate $\lambda_{2,q}$, if we know total variance λ_2, background variance $\lambda_{2,o}$, the mean current, and the single channel amplitude i. The latter may either be known from single channel recordings of receptor channels or else it can be determined by a separate experiment, in which the transmitter is applied to the postsynaptic cell (by ionophoresis, bath perfusion, or local perfusion). When variance from a narrow time window of the recorded current is plotted as a function of mean current, I_p, the desired value for i is the slope of the plot at low I_p (note that the meaning of some of these quantities will be modified below, when we consider filtered signals and when we discuss an alternative for obtaining i).

We are interested in estimating the mean amplitude of the synaptic quantum and its mean frequency of occurrence, ξ. We can obtain both quantities by applying Eq. (1) for the cases $n = 1$ (mean) and $n = 2$ (variance), now considering explicitly the complication due to background noise $\lambda_{2,o}$ and channel noise and also allowing for background current, $I_{p,o}$ and the residual current, I_{res}, originating from residual transmitter (glutamate) in the synaptic cleft:

$$I_p = \lambda_1 = I_{p,o} + \xi h I_1 + I_{res} \tag{6}$$

$$\sigma_I^2 = \lambda_2 = \lambda_{2,o} + i(I_p - I_{p,o}) + \xi h^2 I_2 \tag{7}$$

It is readily seen that the quantities of interest, h and ξ can be calculated from these two equations, if background current $I_{p,o}$, background noise $\lambda_{2,o}$ and the residual current I_{res} (originating from accumulation of cleft transmitter) are either zero or known. The case of vanishing cleft transmitter represents the 'classical' approach as used by many investigators (Del Castillo and Katz, 1954). However, at the Calyx of Held and for many other glutamatergic synapses (Barbour et al., 1994; Carter and Regehr, 2000; Kinney et al., 1997; Mennerick and Zorumski, 1995; Otis et al., 1996; Trussell et al., 1993) $I_{res} = 0$ holds only for very weak stimulation (Borst and Sakmann, 1996), such that alternatives have to be looked for in many measurement paradigms. One alternative is the special deconvolution approach, described below, in which the residual current is estimated by a fit to a simple diffusion model of residual glutamate. Another approach invokes the higher cumulants of the noise fluctuations (Fesce, 1990; Neher and Sakaba, 2001b) in order to obtain additional equations to solve for the additional unknown quantity I_{res}. This is particularly convenient, because it is relatively safe to assume that both background noise and channel noise have a Gaussian amplitude distribution, for which the contributions to the higher cumulants vanish. On the other hand, it is a well-known fact that estimates of higher cumulants are very noisy, such that one needs to average over long stretches of data to obtain reliable values. Keeping this in mind, one can write down the equations for the skewness (λ_3) and for the kurtosis (λ_4):

$$\lambda_3 = \xi h^3 I_3 \tag{8}$$

$$\lambda_4 = \xi h^4 I_4 \tag{9}$$

In theory, it would be easy to solve these two equations for ξ and h:

$$h = \frac{\lambda_4 I_3}{\lambda_3 I_4} \quad \text{and} \quad \xi = \frac{\lambda_3^4 I_4^3}{\lambda_4^3 I_3^4} \tag{10}$$

However, this will work only rarely in practice due to the noisiness of the estimates. For instance, Neher and Sakaba

(2001b) showed by Monte Carlo simulations, that one needs to average over 500 ms of stationary record in order to obtain at best an estimate for ξ with a coefficient of variation of 0.4. This is the case for release rates up to 1 event/ms. The estimates are even worse for higher release rates, since the amplitude distribution approaches a Gaussian with vanishing skewness and kurtosis (see Appendix A) whenever many events overlap. In contrast, the estimates of variance for the same stretch of simulated data had a coefficient of variation smaller than 0.1, which even improved with higher quantal release rates. Thus, one has to carefully consider various aspects of Eqs. (6)–(9) for an optimal solution regarding the quantities of interest. This will depend on the particular circumstances of a given experiment. The relevant factors include length and stationarity of data stretches available, mean frequency of events, and the magnitude of residual current. One approach used by Neher and Sakaba (2001b) was to solve Eqs. (7)–(9) for the single channel current i, according to

$$i = \left(\frac{\lambda_2 - \lambda_{2,o}}{I_p - I_{p,o}}\right)\left(1 - \frac{\lambda_3^2 I_2 I_4}{(\lambda_2 - \lambda_{2,o})\lambda_4 I_3^2}\right) \tag{11}$$

and to apply this to stretches of data, for which release rates are low, but residual current dominates. The late decaying phase of an EPSC following massive stimulation fulfills these requirements. Under these conditions the last term in Eq. (11) is just a small correction to the leading term, such that it is not necessary to determine λ_3 and λ_4 accurately.

Assuming i is constant for a given cell or, at least, for a given record (note the *caveat* in Fig. 1, legend), this value was used for analyzing other sections of the record by solving (6) and (7) for ξ and h, such that

$$h = \frac{\lambda_3 I_2}{\lambda_2 - \lambda_{2,o} - i(I_p - I_{p,o})} \tag{12}$$

$$\xi = \frac{(\lambda_2 - \lambda_{2,o} - i(I_p - I_{p,o}))^3 I_3^2}{\lambda_3^2 I_2^3} \tag{13}$$

This way, one can obtain h and ξ on sufficiently long stationary stretches of data without having to know the contribution

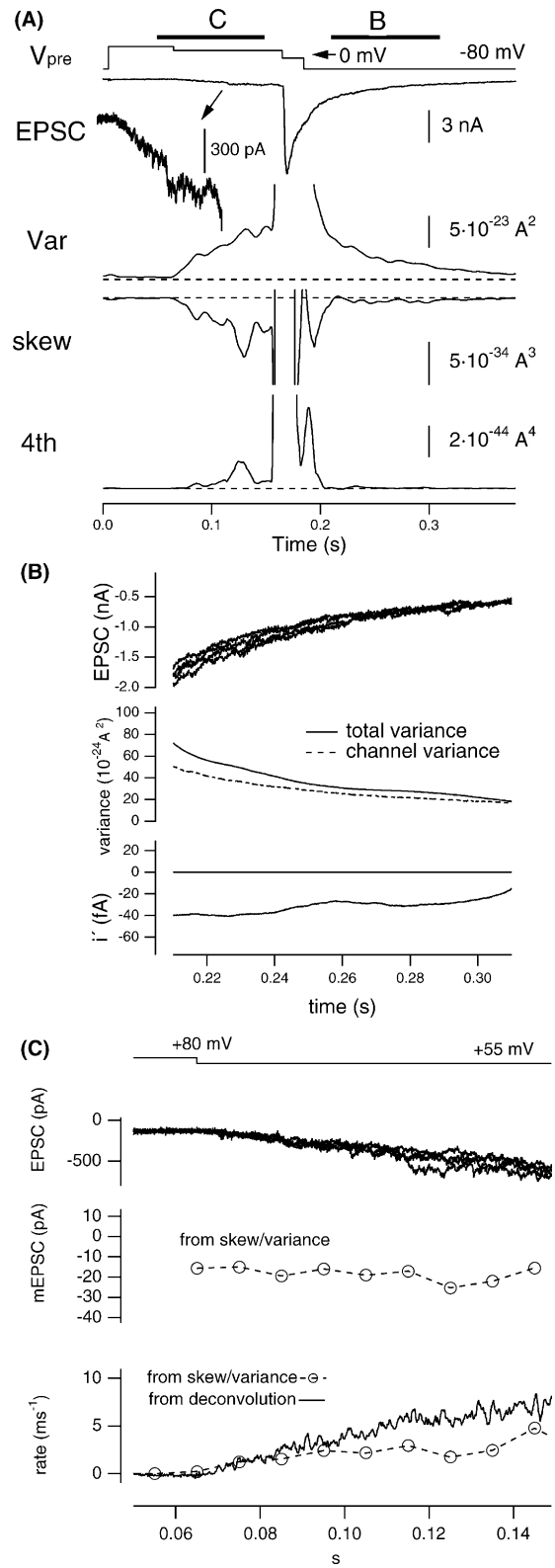

Fig. 1. An example of fluctuation analysis at the Calyx of Held synapse. (A) The presynaptic terminal was depolarized from −80 mV to +80 mV (V_{pre}) and subsequently repolarized to +55 mV (for 100 ms) which evoked slowly rising AMPA-EPSC (moderate release period, see inset). The terminal was subsequently repolarized to 0 mV for 20 ms to deplete available quanta, and finally repolarized to the holding potential (−80 mV). The same protocol was usually repeated 10 times, and variance (variance), skewness (skew) and fourth cumulant (fourth) were calculated after mean subtraction and band-pass filtering. The extracellular solution contained cyclothiazide, an inhibitor of AMPA-receptor desensitization. Modified from Neher and Sakaba (2001b). (B) The late phase of the EPSC (excerpt from time range shown in (A)) is expanded, and variance signal (middle panel) and estimated i' (bottom panel) are plotted. The contribution of channel variance is shown as a broken trace in the middle panel, using an i' value of 30 fA. Note that i' has a tendency to decrease for smaller EPSCs, a feature which is consistently observed. (C) The moderate release period at expanded time scale. mEPSC amplitudes and quantal release rates were calculated according to (B.8) and (B.3) from skewness and variance (middle and the lowest panels, circles with dotted lines). In the lowest panel, release rates estimated from the deconvolution method are superimposed (continuous traces), using the mean mEPSC amplitude of 18 pA, as determined from skew and variance.

of the residual current. Still, estimates which include the skew are noisier than those avoiding it. This is particularly true for estimates of release rates. To calculate the latter, one may therefore try to determine h from a suitable stretch of data and, assuming it is constant (in the absence of postsynaptic desensitization), calculate release rates just from variance, with

$$\xi = \frac{\lambda_2 - \lambda_{2,o} - i(I_p - I_{p,o})}{h^2 I_2} \tag{14}$$

We can see that there is a variety of ways available to look at noise data. Below we will discuss examples and will point out that in practice the analysis should not be performed on the raw data records but on band-pass filtered records. The equations introduced so far hold as well for such band-pass filtered records, except that quantities h, I and I_ν (however not I_p) will have to be reinterpreted as band-pass filtered values. Also, the equations above were simplified in the sense that the dispersion of mEPSC amplitudes was not included. Full equations considering both of these effects are given in Appendix B.

4. Techniques to minimize the adverse effects of non-stationarities

In order to apply Eqs. (6)–(14) one has to evaluate the moments of the signal (e.g. mean and variance) over sufficiently long windows of stationary data, in order to obtain estimates with adequate coefficients of variation (CV). The question is: What is 'sufficiently' long? Neher and Sakaba (2001b) determined CVs for random superpositions of mEPSCs by Monte Carlo simulation and asked the question: How long does the analysis window have to be, in order to achieve adequate CV? It turned out that this 'time resolution' is remarkably good (Table 2 and Fig. 3 of Neher and Sakaba, 2001b). For variance 1–3 ms of recording is sufficient, depending on the mEPSC rate. For the higher moments and the quantities derived from them more averaging is needed; the more, the higher the rate (see below). For instance, for an estimate of h, according to Eq. (12) at 2 events/ms an averaging time of 8 ms is required; for a rate-estimate ξ under the same conditions 40 ms is required (because it involves higher powers of λ_3 and λ_2). In all cases, the analysis was performed on band-pass-filtered signals. The need and benefits of band-pass-filtering was analyzed already by Segal et al. (1985). The need of low-pass filtering is obvious: one does not want to include noise power at frequencies, which are beyond the main components of the mEPSC. The need for additional high-pass-filtering (to define an optimal frequency-band) derives from three arguments:

(1) Campell's theorem requests that the observation interval is long relative to the interval during which the elementary signal is non-zero. mEPSCs decay over several ms, such that without filtering the windows of analysis could not be shorter than about 10 ms. Optimal (matched!) filtering converts an mEPSC into a delta-pulse-like signal, well below an ms, and thus an analysis window of only a few ms is sufficient.
(2) High-pass-filtering effectively removes non-stationarities.
(3) According to the central limit theorem the amplitude distribution of a superposition of independent random events approaches a Gaussian, whenever their number increases beyond a certain value. High-pass-filtering makes the individual events shorter, such that for a given stream of mEPSCs the number of overlapping events is smaller. Thus, the amplitude distribution is less Gaussian, i.e. the skew and kurtosis are, relatively speaking, higher. When designing a high-pass-filter, however, care has to be taken, to preserve the asymmetry of the elementary waveform. Otherwise the skewness will—by definition—be very small.

Some more design principles of filters are discussed in Neher and Sakaba (2001b). Fortunately, all equations derived so far apply equally well to filtered signals. The only change with respect to what was written so far is that the quantities $I_1, \ldots, I_4$ have to be evaluated as time integrals over the filtered signals. Likewise, the single channel amplitude is no longer a 'real' amplitude, but that of the filtered single channel current. In the equations given by Neher and Sakaba (2001b) and in Appendix B this is indicated by a prime, which is a superscript for all quantities in question (such as $I'_1, I'_2, \ldots, I'$).

In practice, the following steps are required for a fluctuation analysis as described in Neher and Sakaba (2001b):

(1) Series resistance compensation of postsynaptic voltage-clamp traces. This is important, because relative clamp errors increase with the nth power of the cumulant order.
(2) Software band-pass-filtering.
(3) Calculation of moments and cumulants on a sliding data window. The data window has to be long enough, such that the CV of all relevant moments and cumulants is $\leq 1/3$ (otherwise errors will explode, when forming ratios, etc.).
(4) Calculation of the parameters of interest, using appropriate calibration constants (see Appendix B).

Calibration constants: I_ν-values and moments of the amplitude distribution can either be calculated on the basis of the known mEPSC time course and amplitude distribution after band-pass-filtering or else be determined by Monte Carlo simulation. Software, which performs the analysis, is available on our department's website: http://www.mpibpc.gwdg.de/abteilungen/140/software/index.html.

So far, the analysis was described for the case that only a single record of a given type is available. High-pass-filtering was the only means considered to remove non-stationarities and trends. Results can be very much improved, when several records of similar time course are available (for

instance several traces with slowly decaying asynchronous mEPSCs after stimulation). This allows averaging the estimates from individual records and further elimination of non-stationarities by mean-subtraction. Mean subtraction can be performed in several ways. For the calculation of variance it is most convenient to subtract consecutive records from one another before applying the analysis. The variance of such difference records is twice the variance of a single record. It can be shown that averaging estimates of variances from all possible consecutive difference records (interleaved differences!) results in an estimate almost as good as subtracting individual records from the mean-record (Scheuss and Neher, 2001; Sigworth, 1980). At the same time slow trends are eliminated much more effectively by this method. Unfortunately, the same procedure cannot be applied for skewness, because skewness is canceled out by subtraction. However, subtraction of individual traces from the mean is quite effective, if five or more traces are available. The combination of mean subtraction and high-pass-filtering makes it possible to handle non-stationarities remarkably well, as shown by Neher and Sakaba (2001b) in simulations.

5. Examples of fluctuation analysis at a glutamatergic synapse

Fig. 1A shows an example of the analysis at the Calyx of Held synapse. The presynaptic terminal was depolarized to +80 mV and subsequently repolarized to +55 mV for 100 ms to induce a slowly rising EPSC (moderate release period). Subsequently, the terminal was held at 0 mV for 20 ms to evoke massive release. As the terminal was clamped back to −80 mV, the EPSC decayed slowly. The same stimulation protocol was applied 10 times, and variance, skewness, and fourth cumulants were calculated over a sliding window of 10 ms length for each trace after mean-subtraction and band-pass-filtering (see above). Variance, skewness, and fourth cumulant were averaged over the 10 traces. They increase slowly during the moderate release period, suggesting that release rates increase slowly. However, the fluctuations in skew and fourth cumulant are too large to reliably estimate release rates and mEPSC amplitudes from Eq. (10) (or (B.7) and (B.11)). During the depolarization to 0 mV, all three traces are truncated in the figures, because the rapid rise and fall of EPSCs introduces strong non-stationarities, which cannot be removed completely by mean-subtraction and band-pass-filtering in this experiment. After repolarization to −80 mV, the variance decays with similar time course as the EPSC, whereas skewness and fourth cumulant decay more rapidly. This indicates that quantal release rates rapidly decrease to zero, and that the remaining variance is mainly composed of AMPA-receptor channel variance. In other words, the late EPSC is a consequence of the delayed clearance of transmitter at the synaptic cleft. Such a qualitative use of higher cumulants may help to judge the presence of 'spill over' and to distinguish it from asynchronous release (Barbour and Häusser, 1997).

However, a more quantitative analysis is possible: using the decay phase of the EPSC, the single channel amplitude i' was calculated according to Eq. (11). Fig. 1B shows the EPSC, the variance, the contribution of channel variance to total variance (Eq. (B.14) of Appendix B), and i' in the time window between 0.21 and 0.31 s (indicated by the bar). It is seen that i' is quite constant in this time window (although there is some trend to decrease with decreasing EPSC, which is observed consistently). Since the EPSC covers about the same range of values as the EPSC in the early 'moderate release period' of Fig. 1A we can use the estimated value of i' to subtract channel variance from total variance. Fig. 1C (upper panel) shows the superimposed EPSC traces during the moderate release period. We use Eqs. (12) and (13) (or (B.3) and (B.9)) to calculate the mEPSC size and quantal release rates (middle two panels). For comparison, release rates as estimated from the deconvolution method (described below) are also shown in the lowest panel of Fig. 1C. During the 'moderate release period', the quantal amplitude is estimated to be around 20 pA, and it stayed constant. This value is within the range of those for spontaneously occurring mEPSCs (20–40 pA). Release rates increase slowly during the moderate release period, finally up to 5 m/s (for details, see Neher and Sakaba, 2001b). Although estimates from the deconvolution method tend to be larger, both methods (skew/variance and deconvolution) give similar results. The type of analysis, presented here, is not restricted to synapses, in which the terminal can be voltage-clamped. In fact, it is straightforward to determine the cumulants during episodes of asynchronous release following trains of afferent nerve stimulation and to calculate mEPSC amplitudes and rates as a function of time after the train, as will be discussed below.

6. Non-stationary noise analysis of evoked responses

The approach, described above started from the analysis of stationary stretches of data. We showed that high-pass-filtering and mean-subtraction allows this approach to be extended in a remarkable way to non-stationary cases as well. Synaptic responses, evoked by afferent nerve stimulation represent an extreme case of non-stationary. It should be possible to extend the approach described above to ensembles of evoked responses the same way Sigworth (1980) extended fluctuation analysis of voltage clamp Na^+-current records to the extreme case of step depolarization evoked responses. Traditionally, however, in synaptic physiology the analysis of nerve-evoked responses is restricted to measure peak values of repetitively evoked composite EPSCs and to consider these as representing the fluctuating number of released quanta. Elaborate techniques are available to extract the quantal parameters from such fluctuations by analyzing stretches of stationary data (i.e. records for which the mean peak amplitude keeps constant

over many repetitions). Here, we will shortly discuss two aspects of such an analysis: (i) the slight asynchrony of quantal release and the extent to which it compromises the assumption that the peak EPSC represents the number of released quanta and (ii) the technique of non-stationary mean–variance analysis, in which trains of stimuli are applied repetitively and covariance between successive stimuli within trains is analyzed in addition to the variance. This technique allows separate estimations of changes in the quantal parameters q and m, which occur during such trains (Scheuss and Neher, 2001; Scheuss et al., 2002).

6.1. Asynchrony of release in quantal analysis

It is generally assumed in quantal analysis that the peak of an evoked EPSC represents the number of released quanta and that the mean amplitude of a single quantum is the ratio of the peak amplitude over the number of quanta. This is true, however, only when release is ideally synchronized or else if the jitter in release is much smaller than the decay time of the mEPSC, conditions, which are not exactly met at the Calyx of Held. Borst and Sakmann (1996) showed that the distribution of quantal delays at low external [Ca^{2+}] has a width of about 1 ms, which is appreciably longer than the rise time of mEPSCs and comparable to the decay time. Thus, the peaks of the mEPSC will not all contribute maximally to the peak EPSC and those starting after the peak of the EPSC will be neglected altogether. To interpret the variance of the peak readings, one has to ask what fraction of their peak amplitudes individual mEPSCs contribute at the time of the peak EPSC. If the latency distribution and the time course of mEPSCs is known, the distribution of such fractional numbers can be calculated and convolved with the amplitude distribution. The coefficient of variation of this modified amplitude distribution should then be used to calculate the correction factor for amplitude dispersion. Also, one can calculate how much the peak EPSC is attenuated by calculating release rates as a function of time by one of the fluctuation methods described above (or else by deconvolution of the evoked response, as described below) and convolving these with the mEPSC waveform. This is shown in Fig. 2, where this problem is analyzed by Monte Carlo simulation. The lower trace is the time course of release rate as typically observed by deconvolution of nerve-evoked EPSCs (e.g. Schneggenburger and Neher, 2000). The continuous upper curve is its reconvolution with the mEPSC, which reproduces the EPSC. The two broken lines, marked ‘1’ and ‘2’, are convolutions of delta functions with the mEPSC, i.e. EPSCs that would be expected if all mEPSCs were ideally synchronized. Those broken curves differ in the number of mEPSCs assumed. In curve ‘1’ all mEPSCs are included. Curve ‘2’ includes all mEPSCs which start up to the peak of the EPSC. This example shows that the peak of the measured EPSC is only about 85% of what it would be in the case of ideal synchronization of vesicles (or about 90% if only mEPSCs up to the peak are counted).

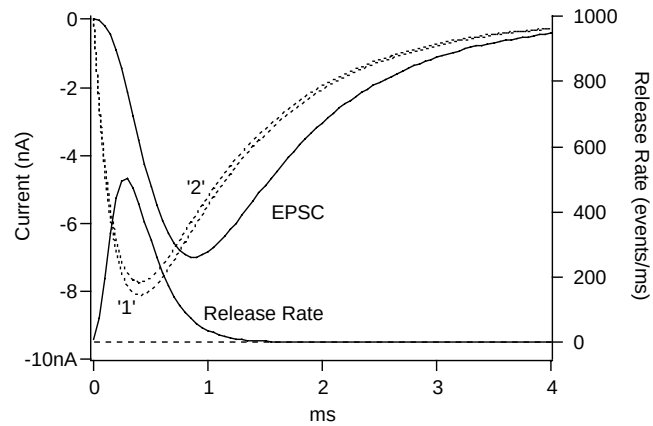

Fig. 2. Simulation of asynchrony within EPSCs. EPSCs were simulated assuming an mEPSC of 32 pA amplitude, with 0.2 ms rise time constant and 1 ms decay time constant (90%). A second slow decay (10%) had 10 ms time constant. The trace ‘EPSC’ (left ordinate) was simulated using the release rate function as displayed (right ordinate). As a template for ‘release rate’ a lognormal function with a halfwidth of 0.44 ms was used, which is very similar to experimental release rates. It was scaled such that the total release (its integral) was 250 vesicles. Trace ‘1’ was simulated using a delta function comprising 250 vesicles at time zero as release rate. Trace ‘2’ was simulated using another delta function comprising 238 vesicles. This is just the number of vesicles, which is released during the EPSC up to the time of its peak.

6.2. Non-stationary mean variance analysis

Some of the most interesting questions of quantal analysis are connected to short-term plastic changes during trains of stimuli. If facilitation or depression is observed, one would like to know whether this is due to postsynaptic changes (such as desensitization, which most likely would show up as a change in q) or else due to changes on the presynaptic side (which may result in a change in quantal content). Ideally one would like to estimate q and m for each response in a train. For this purpose, the mean–variance approach, as described by Silver et al. (1998) and Clements (2003) can be extended by applying it to repetitive trains of pulses. Enough time has to be allowed between trains for the synapse to recover completely. Then, means ($\bar{y}_\nu$) and variances ($\sigma^2_{y,\nu}$) of all EPSCs in the trains can be calculated individually for each ν (ν = number of EPSC within train). Plotting $\sigma^2_{y,\nu}$ against $\bar{y}_\nu$ will result in a parabola, from which quantal size q and the binomial parameters N and P can be determined, if

- q is constant for all stimuli,
- a large enough range of release probability is covered within the train, and
- the vesicle population is homogeneous.

Oleskevich et al. (2000) and Reid and Clements (1999) applied this technique to pairs of pulses and to trains at various frequencies. They described deviations from the parabola, which were interpreted to indicate changes in q as a result of desensitization. Meyer et al. (2001) used the technique at

the Calyx of Held, to study the influences of both desensitization and saturation of postsynaptic receptors on the fluctuations. They showed that cyclothiazide (CTZ) can protect from desensitization for short times and that the binomial parameter N may be an upper limit estimate for the number of active zones. A systematic Monte Carlo study of the influences of desensitization, saturation and heterogeneity in release probability on variance and mean estimates was performed by Scheuss and Neher (2001). They considered a model of short-term depression in which depression can be the result of either receptor desensitization or depletion of a pool of release-ready vesicles. To this purpose they assumed the release probability p to be a product of vesicle availability p_a, reflecting the occupancy of a given release site and p_r, the probability of release of an available vesicle. In such a model, all the quantities measurable by fluctuation analysis depend only on the product $p_a p_r$ and not on the probabilities individually, such that, unfortunately, these quantities cannot be determined individually (see also Vere-Jones, 1966; Quastel, 1997). However, the study of Scheuss and Neher (2001) showed that under certain conditions consideration of covariance between subsequent responses within trains together with mean–variance analysis allows estimates of the quantal parameters q_ν and m_ν for each stimulus number ν within trains individually (even if q_ν and m_ν change during a train). In this formulation, m_ν is the product of p_a, p_r, and the number of release sites N.

If the frequency of stimulation within trains is high enough, such that only little recruitment of vesicles occurs between pulses and if no mechanisms other than pool depletion contribute to covariance, then the quantal size q_ν^* for the νth stimulus in a train is simply given by (Scheuss and Neher, 2001)

$$q_\nu^* = \frac{\mathrm{Var}_\nu}{\bar{I}_\nu} - \frac{\mathrm{Cov}_{\nu,\nu+1}}{I_{\nu+1}} \tag{15}$$

Here, Var_ν and I_ν are variance and mean of the νth response, $\mathrm{Cov}_{\nu,\nu+1}$ is the covariance between responses ν and $\nu+1$, and the asterisk ($*$) denotes that the value is not corrected for dispersion of mEPSC amplitudes. The first term in this equation (which is equal to the initial slope of a variance–mean parabola) is the well-known result for the case of low p. The second term can be considered as a correction, which becomes larger, when p is increased. This is intuitively clear, since correlation between two consecutive responses (within the framework of the model considered) arises from depletion of the pool of releasable vesicles, which happens only when p is substantial (note that p is the product of p_r and p_a). Unfortunately, mechanisms other than pool depletion may contribute to such correlations, such as postsynaptic receptor desensitization and saturation. Both of these mechanisms will result in negative correlation, just as pool depletion does. Thus, the measured covariance may represent an overcorrection, if used in Eq. (15) and the equation can only provide an upper and lower bound to q_i^*, if used with and without the correction term, respectively. However, in the analysis of Scheuss et al. (2002) it turned out that the covariance term was small relative to the first term for all responses in the train, except for the first one. This is because depression, which was already prominent for the second pulse, reduced p sufficiently. Thus, the covariance term in Eq. (15) can be considered as an indicator whether or not the low-p limit has been reached. A caveat has to be added at this point: this conclusion will not hold in the case that negative correlation resulting from the mechanisms considered above is canceled by positive correlation produced by some other mechanisms.

Fig. 3 reproduces some of the results of Scheuss et al. (2002). Details of the experiment are given in the figure legend. The analysis showed that in the control case (without drugs) the quantal size q^* was reduced by almost a factor of 2 for the second pulse in a train (Fig. 3D). For the first response the covariance term increased the q_1^* estimate by about 50%, if fully applied, and the resulting value was slightly larger than the value measured independently from spontaneously occurring mEPSCs. The uncorrected q_1^* estimate, on the other hand, was lower than the mEPSC-derived value. It was concluded that probably some of the observed covariance was of postsynaptic origin. Experiments were also performed in the presence of CTZ and kynurenic acid (Kyn), two drugs, which are known to delay desensitization and to prevent receptor saturation, respectively. As expected, the decrease in q^* during trains was much less in CTZ alone, and virtually disappeared in the presence of both drugs (Fig. 3D). The q_i^* values were used together with mean EPSC values to calculate the quantal content (Fig. 3E). This revealed a presynaptic action of CTZ in the form of an increase in quantal content, which was particularly prominent for the second and third pulse in a train.

7. Deconvolution and fluctuation analysis

The advantage of voltage-clamping the presynaptic terminal can be fully exploited only if a method is at hand to extract rates of transmitter release from the postsynaptic current. For any presynaptic depolarization lasting longer than an action potential the problems of asynchrony in release, discussed above, will seriously blur the interpretation of EPSCs. The standard method to calculate release rates from postsynaptic currents is deconvolution (Aumann and Parnas, 1991; Borges et al., 1995; Diamond and Jahr, 1995; Van der Kloot, 1988a, 1988b; Vorobieva et al., 1999). Unfortunately, the method cannot be applied in its usual form to the Calyx due to the presence of ‘residual current’—a current resulting from glutamate accumulating in the synaptic cleft—whenever stimulus-strength or duration exceeds certain limits. However, a major advantage of a voltage-clamped presynaptic terminal is exactly the ability to apply strong stimuli, because this allows one to deplete vesicle pools at the end of a stimulation protocol, such that earlier responses can be related to the number of remaining vesicles.

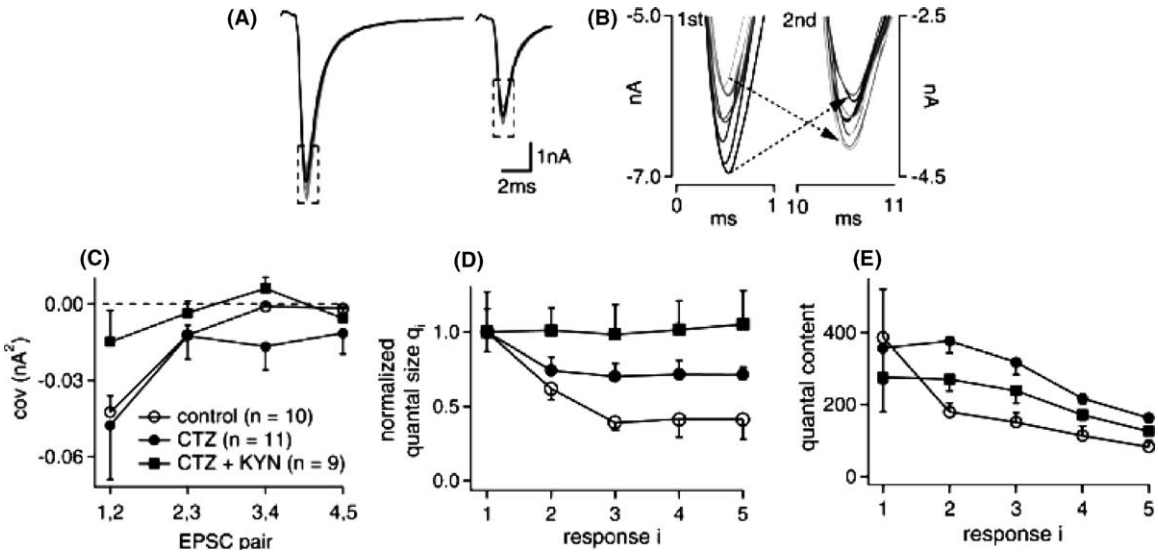

Fig. 3. Covariance analysis at the Calyx of Held. (A) The nerve-fiber was stimulated extracellularly with a frequency of 100 Hz, and the postsynaptic principal neuron was whole-cell clamped at −80 mV. Nine example traces of first and second EPSCs in a train from consecutive sweeps (gray) and their mean (black) are shown. (B) Correlation between the amplitudes of the consecutive EPSCs are shown. Arrows identify traces belonging to the same train. (C) Average covariance in the amplitude of consecutive EPSCs in the five stimulus trains (100 Hz) are shown. Experiments are done under three conditions; control, in the presence of CTZ (cyclothiazide), in the presence of CTZ and Kyn (Kynurenic acid). Covariance between the first two responses in trains is significantly different from zero. (D) Plot of the average quantal sizes estimated from the covariance method. Same symbols as shown in part C. (E) Plot of the average quantal content estimated from the covariance method. Same symbols as in part C. From (A) to (E), modified from Scheuss et al. (2002).

The basic assumption of the deconvolution method is that the measured response is a linear superposition of a certain number of elementary events. This assumption is violated whenever 'residual current' develops. The method of deconvolution that we have developed and used for all of our voltage-clamp studies at the Calyx of Held solves this problem by incorporating a simple model of glutamate diffusion in the synaptic cleft into the deconvolution algorithm. The role of the diffusion model is to estimate for a given time point along the EPSC trace the residual current, based on the preceding release. This current is subtracted from the measured EPSC and the remaining current is deconvolved. The diffusion kernel and the mEPSC time course have to be known for a given synapse. We usually represent the mEPSC time course by a function decaying with one or two exponential components and include the time constant(s) of decay and, if applicable, the relative size of the components among the fitting parameters. The diffusion kernel involves a mean diffusional distance r_D, a diffusion coefficient D, and an exponent n_D. The rationale for the approach is given in Neher and Sakaba (2001a). Unfortunately, the equations for the diffusion kernel given both in Sakaba and Neher (2001) contain misprints. The correct formula, which was used in the calculations in both papers is, therefore, given here. The kernel $c(t)$, which enters into Eq. (3) of Neher and Sakaba (2001a) is

$$c(t) = \frac{\text{const}}{t^{n_D}} \exp\left(\frac{-{r_D}^2}{4Dt}\right), \tag{16}$$

where 'const' is part of a fitting parameter, which scales the contribution of the residual current. In total, up to six parameters have to be determined for a given synapse. This may appear to be a difficult task. However, it can readily be solved with the help of fluctuation analysis and a suitable 'fitting protocol', which we routinely apply a few times at the beginning and the end of a recording session. Applying the 'fitting protocol' periodically also helps to check stability of the recording. In the following we describe this fitting protocol, while at the same time explaining some aspects of the diffusion model. More detailed descriptions of the procedures can be found in Neher and Sakaba (2001a) and in a help text, which can be downloaded together with analysis programs (in IGOR) from our department's webpage (http://www.mpibpc.gwdg.de/abteilungen/140/software/index.html).

A 'fitting protocol' typically starts with a very short episode of Ca^{2+} influx, which is adjusted such that it elicits not more than about 1–2 nA in postsynaptic current (Fig. 4). This stimulus is followed by pauses and further episodes of Ca^{2+} influx of increasing duration. The whole fitting protocol is typically 300 ms in length. We deconvolve this record with a set of default starting parameters and first concentrate on the deconvolution result during and following the first short depolarization. During this episode the parameters describing the glutamate accumulation/diffusion process should not matter, since little glutamate has been released. Indeed, it has been shown that EPSCs under such conditions are well represented by linear summation of mEPSCs (Borst and Sakmann, 1996). If the mEPSC parameters are correct, the deconvolution result should be a short pulse, returning to base line within about an ms after the end of the depolarization, since little asynchronous release is elicited by the first depolarization. We confirm the ab-

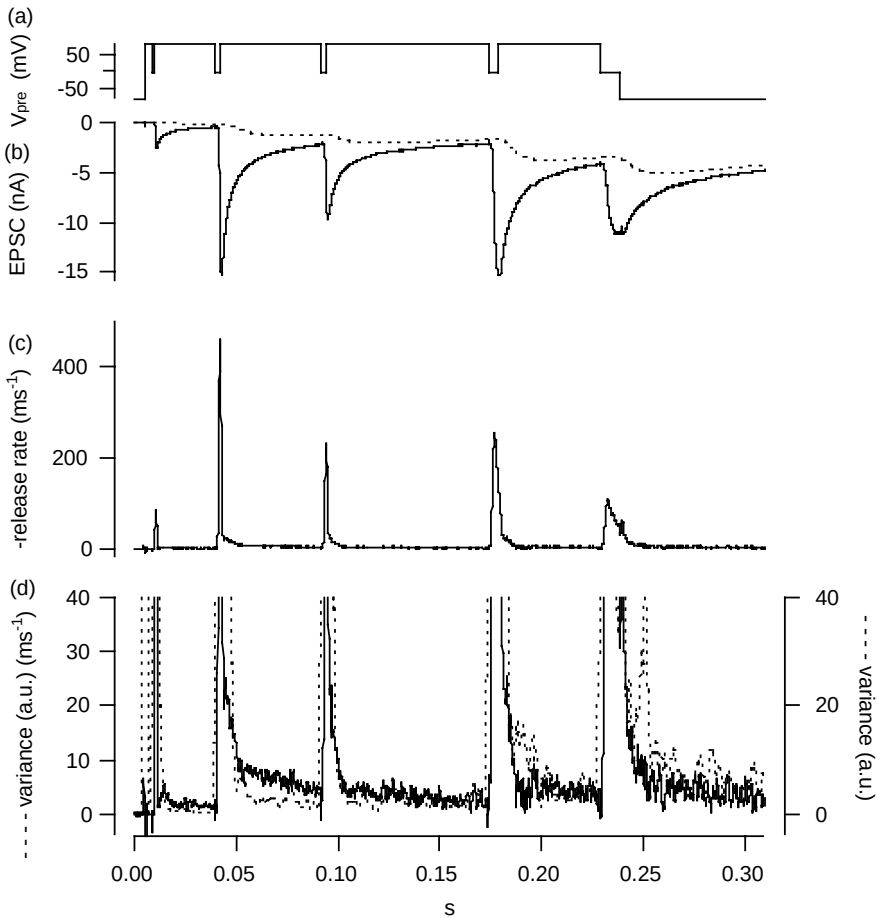

Fig. 4. Fitting protocol for the deconvolution method. The presynaptic terminal was depolarized from −80 to +80 mV (a), and periodically repolarized to 0 mV with different durations to evoke EPSCs with different amplitudes (b). At the end of the protocol, the terminal was held at 0 mV for 10 ms, to deplete the releasable pool. The residual current due to delayed clearance of glutamate from the synaptic cleft (dotted trace superimposed on the EPSC) was estimated from the diffusion model. This current component was subtracted from the original EPSC and the remaining current component was deconvolved with the mEPSC in order to estimate quantal release rates (c). In (d), fluctuation (variance) analysis was used to check whether release rates drop to a low level in between pulses. Calculated variance was scaled according to Eq. (B.1) assuming that quantal size is the same as that of spontaneously occurring mEPSCs. We designate the value as arbitrary unit (a.u.) of variance (dotted trace, right axis). Release rates estimated from the deconvolution method (left axis) were superimposed, such that signals of similar amplitude (1 vesicle m/s and 1 a.u.) are expected. From Neher and Sakaba (2001a).

sence of asynchronous release by performing a fluctuation analysis according to Eq. (B.1) on the episode between the first two pulses. Usually slight adjustments of mEPSC parameters are necessary to match the deconvolution with the fluctuation results. It should also be noted that estimated release rates from the deconvolution method are less sensitive to mEPSC parameters if mEPSCs decay slowly (Eq. (7) of Neher and Sakaba, 2001a), which is the case in the presence of CTZ. Subsequent stimulation episodes are stronger and elicit large EPSCs, residual current (see broken line in part b), and also some degree of asynchronous release. We measure asynchronous release in episodes between pulses by fluctuation analysis and adjust the remaining fitting parameters, such that the deconvolution result during these episodes agrees with the fluctuation result (Fig. 4d). This, in effect, constitutes a fit of the diffusion parameters to the residual current on all these episodes. The assumption underlying our method is that this fit faithfully interpolates the release episodes in between stimuli. The amount of asynchronous release during the decay phase of EPSCs should be kept small in the fitting protocol, in order to estimate residual current precisely (it will be ideal if the EPSC decay consists only of the residual current). At the same time, EPSC amplitudes during the fitting protocol must cover the whole range of EPSC amplitudes, which will be encountered in the experiment to be analyzed. Because residual current is a supra-linear function of the amount of transmitter release, deconvolution of EPSCs, which are larger in amplitude than those of the fitting protocol, leads to serious errors in the outcome. At the Calyx of Held, the duration of the presynaptic depolarizing pulses was adjusted so that EPSCs in the fitting protocol cover a wide range of amplitudes. The presynaptic terminal was held at −80 mV or +80 mV in between pulses to evoke little asynchronous release. In the case of an unclamped presynaptic terminal (as in many other synapses), a train of nerve stimulations

can be used for fitting the deconvolution parameters. In that case, it is also recommended to combine deconvolution with fluctuation analysis to check independently the amount of asynchronous release.

At the Calyx of Held, the parameters for the deconvolution method usually are (under CTZ):

- Time course of mEPSCs (under CTZ): $\tau_{fast} = 2–3$ ms (30–50% of the total), $\tau_{slow} = 10–20$ ms.
- n (exponent of the glutamate channel activation) = 1.2–1.4.
- n_D (exponent of the glutamate diffusion) = 0.6–0.8.
- Diffusion distance: 2–3 μm.
- D (diffusion coefficient of glutamate): 30 μm^2/s.

Release rates in Fig. 4 are calculated using such parameters, and it can be seen that residual current (due to glutamate accumulation, broken line in Fig. 4b) develops slowly, and mainly contributes to the late phase of EPSCs, consistent with the observation at other Calyx synapses (Otis et al., 1996).

8. Outlook

Deconvolution and fluctuation analysis complement each other in an ideal way. Deconvolution gives best results for large, rapidly changing EPSCs. In fact, if mEPSCs were step-like functions with decay times much longer than rise times the deconvolution result would be just the time derivative of the EPSC with a small correction due to the mEPSC decay (Van der Kloot, 1988a). Fluctuation analysis, on the other hand, is most readily performed on relatively stationary stretches of small amplitude postsynaptic currents, although mean subtraction and band-pass-filtering can effectively eliminate the adverse effects of non-stationarities. For this, however, several repetitions of a given record have to be available. When considered together, results from deconvolution and the various forms of fluctuation analysis constitute powerful tools to dissect influences of residual glutamate, asynchronous release, and postsynaptic changes, such as desensitization and saturation of receptors. Among the latter, the role of saturation has drawn the least attention so far (but see Meyer et al., 2001). In some of our work, we used kynurenic acid, a low affinity antagonist to avoid saturation. However, this approach has very adverse effects on fluctuation analysis, since variance, skew and kurtosis decrease with the square, third, or fourth power of the blocking factor, respectively. A better way to handle saturation may be to explicitly adopt a suitable dose–response curve for the agonist to the algorithms for deconvolution and for interpreting fluctuation results. This will, of course, introduce new parameters, such as a dissociation constant and the saturation level. On the other hand it may provide information on the properties of the postsynaptic receptors.

The methods we describe should be readily applicable to other synapses, although our own experience, so far, is restricted to the Calyx of Held. This should be particularly true for the fluctuation analysis part, which was originally formulated by Fesce (1990) for the neuromuscular junction. We extend this treatment here to include 'residual glutamate' in the synaptic cleft and the resulting 'residual current'. This problem is particularly severe for relatively young calyces. The contribution of residual current may be much reduced at more mature synapses (Joshi and Wang, 2002; Taschenberger et al., 2002) and may be negligible at many types of synapses. In these cases, our equations can be used by simply setting i' to zero. The correctness of this simplification may be checked by varying i' within a reasonable range (note that i' is a band-pass-filtered single channel current) and verifying that the expected contribution of any residual current to variance is negligible. For calculation of the calibration constants (Eqs. (B.2), (B.4), (B.6), (B.10) and (B.12)) information on the amplitude distribution and mEPSC time course is required for a given synapse. In our programs, this is supplied by measured mEPSC amplitude distributions and by specifying the risetime and decay time constants of mEPSCs. However, these quantities might be replaced by reasonable assumptions—at some loss of accuracy in absolute numbers—in case the mEPSCs cannot be measured at a given synapse. With such assumptions and neglecting residual current Eqs. (B.3) and (B.9) should be applicable to many types of synapses for the measurement of both mEPSC mean amplitude and release rate (as functions of time) during episodes of asynchronous release after evoked responses or for spontaneous release.

The deconvolution procedure, as described here, strongly relies on the 'fitting protocol', which requires that the presynapse can be voltage-clamped. However, again, the main problem at the Calyx of Held is 'residual current' which may be much less at other synapses. When residual current is only a minor contribution, it is well conceivable that the remaining fitting parameters (time constants of the mEPSCs) can either be predetermined or else fitted in a protocol where short bursts of nerve evoked EPSCs replace the depolarizations, which we use for the voltage-clamped terminal. Then self consistent release rates and mEPSC amplitudes can be derived from the combined analysis of deconvolution and variance according to Eqs. (B.8) and (B.8a) (with $i' = 0$ and the weighing factor β of Eq. (2) in Neher and Sakaba (2001a) set to zero). All the calculations described here should, of course, be equally applicable to IPSCs. We expect the approach to be particularly helpful for analyzing IPSCs, because asynchronous release is very prominent in many inhibitory synapses (Lu and Trussell, 2000).

Acknowledgements

We thank Volker Scheuss for discussions and Holgar Taschenberger for comments on the manuscript. This work is supported in part by a grant of the Deutsche Forschungsgemeinschadt (DFG) to E.N. (SFB 406).

Appendix A. Some principles of statistics

Some basic principles regarding random variables are repeatedly used throughout this chapter. Detailed discussions of these can be found in textbooks on basic statistics, such as Spiegel (1975), Bevington (1969) and Kendall (1947) (see also Fesce, 1990; Heinemann and Sigworth, 1991). A short summary is given here.

A.1. Additivity of cumulants (or semi-invariants)

If two or more random variables are statistically independent from each other, then the cumulant of the sum of these variables is equal to the sum of the cumulants. This theorem is well-known to hold for the mean and the variance, but it also holds for skewness, kurtosis and other cumulants (also called semi-invariants). Cumulants, λ_n, are defined in terms of moments μ_n of random variables. If μ_n is the nth moment of the function $f(x)$, according to

$$\mu_n = \int_{-\infty}^{+\infty} f(x)^n \, \mathrm{d}x \tag{A.1}$$

then the cumulants λ_n are given by (for simplicity we write the equations for high-pass-filtered or mean subtracted traces):

$$\lambda_1 = \mu_1 = 0 \quad \text{(mean)} \tag{A.2}$$

$$\lambda_2 = \mu_2 \quad \text{(variance)} \tag{A.3}$$

$$\lambda_3 = \mu_3 \quad \text{(skewness)} \tag{A.4}$$

$$\lambda_4 = \mu_4 - 3\mu_2^2 \quad \text{(kurtosis)} \tag{A.5}$$

In electrophysiology, this law is readily applied to random signals, for instance currents originating from N independently switching channels or N independently releasing active zones. For these one can write

$$\lambda_{2,N} = N\lambda_2 \tag{A.6}$$

$$\lambda_{4,N} = N\lambda_4 \tag{A.7}$$

where $\lambda_{2,N}$ and $\lambda_{4,N}$ are the cumulants of the recorded currents, whereas λ_2 and λ_4 are cumulants of single channel (or single active zone) signals. Note that such a simple equation does not hold for the raw fourth moment ($\lambda_4 = \mu_4 - 3\mu_2$)!! and that they hold for variance and skewness only for mean-subtracted traces.

A.2. Multipliers to random variables

If a random variable $f_2(x)$ is a scaled version of another random variable $f_1(x)$, according to

$$f_2(x) = \alpha f_1(x) \tag{A.8}$$

then the cumulants $\lambda_{n,2}$ of $f_2(x)$ are related to those, $\lambda_{n,1}$ of $f_1(x)$ by

$$\lambda_{n,2} = \alpha^n \lambda_{n,1} \tag{A.9}$$

A.3. The cumulants of Gaussian noise

A Gaussian distribution has very special properties with respect to its cumulants, especially if we consider high-pass-filtered (or mean-subtracted) signals: all its cumulants, except for the variance, vanish. Therefore, the Gaussian is completely characterized by the variance (λ_2). The fact that the skewness vanishes is a simple consequence of its symmetry. The fourth cumulant (kurtosis) vanishes because the fourth moment μ_4 of a Gaussian is $3\lambda_2$ (see definition of kurtosis above).

A.4. Higher cumulants of superpositions of many random events

Higher cumulants are only useful for 'sparse' signals, i.e. signals for which only a small number of random events superimpose. This is because of the 'central limit theorem', which states that the statistical distributions of superpositions of independent random variables approach Gaussian distributions, when the number of superimposing events increases. Together with the general result (above) that higher moments of Gaussians vanish, this leads to very unfavorable conditions for the analysis of higher moments, when the frequency of elementary events increases.

Appendix B. Summary of equations

Here, we summarize equations for estimating mean amplitudes $\langle h \rangle$ of synaptic quanta and rates of release $\langle \xi \rangle$ of quanta from cumulants. $\langle \xi \rangle$ and $\langle h \rangle$ can be considered as time-dependent, since they are usually evaluated on short windows, which slide along data records. Most of these equations are from Neher and Sakaba (2001b), where, however, they were given without correction terms for offset current and background variance. Some equations are derived in the text (Eqs. (6)–(13)), however, without the complication of the dispersion in mEPSC amplitudes.

B.1. Meaning of symbols

A prime notifies the fact that high-pass-filtered or mean-subtracted quantities have to be used.

- $\langle h \rangle$ mean amplitude of elementary quanta (mEPSCs) in amperes ($\langle h^2 \rangle$, $\langle h^3 \rangle$ and $\langle h^4 \rangle$ are the higher moments of the amplitude distributions)
- $\langle \xi \rangle$ mean frequency of occurrence of quanta within a short analysis window. This quantity should be considered as a function of time of the window in most cases
- λ_2' the variance after band-pass-filtering of the current record
- λ_3' the skew after band-pass-filtering of the current record

λ'_4 the fourth cumulant (also called fourth semi-invariant or kurtosis) after filtering
i' the apparent single channel conductance after filtering. See Eq. (B.15) for its definition
I_p the measured postsynaptic current before band-pass-filtering (possibly low-pass-filtered)
$I_{p,o}$ the offset of the postsynaptic current, which is not related to synaptic transmission, including leak-current
$\lambda'_{2,o}$ the background variance of the postsynaptic current after filtering, including amplifier noise and cellular background noise
I'_2 the integral over the square of the peak-normalized mEPSC waveform after filtering
I'_3 the integral over the third power of the peak-normalized mEPSC waveform after filtering
I'_4 the integral over the fourth power of the peak-normalized mEPSC waveform after filtering
H'_v a calibration factor used in the conversion of variance into mEPSC amplitude and rates. See Eq. (B.2) for its definition
H'_s a calibration factor used in the conversion of skew into mEPSC amplitude. See Eq. (B.10) for its definition
H'_4 a calibration factor used in the conversion of the fourth cumulant into mEPSC amplitude. See Eq. (B.12) for its definition
Z'_s a calibration factor used to convert skew and variance into release rates. See Eq. (B.4) for its definition
Z'_4 a calibration factor used to convert skew and the fourth cumulant into release rates. See Eq. (B.6) for its definition

B.2. Calculating release rates

B.2.1. From variance, applying corrections for background variance ($\lambda'_{2,o}$), channel variance, and offset current $I_{p,o}$

$$\langle\xi\rangle = (\lambda'_2 - \lambda'_{2,o} - i'(I_p - I_{p,o}))\frac{H'_v}{\langle h\rangle^2} \tag{B.1}$$

$$H'_v = \frac{\langle h\rangle^2}{\langle h^2\rangle I'_2} \tag{B.2}$$

This calculation requires knowledge of the absolute mEPSC amplitude (see Eq. (B.8a), for a calculation of $\langle\xi\rangle$ using variance and deconvolution).

B.2.2. From skew and variance, applying corrections for background variance, channel variance, and offset currents

$$\langle\xi\rangle = \frac{(\lambda'_2 - \lambda'_{2,o} - i'(I_p - I_{p,o}))^3}{\lambda'^2_3}\cdot Z'_s \tag{B.3}$$

$$Z'_s = \frac{\langle h^3\rangle^2}{\langle h^2\rangle^3}\frac{I'^2_3}{I'^3_2} \tag{B.4}$$

For this calculation knowledge of mEPSC amplitude is not required; however the ratio $\langle h^3\rangle^2/\langle h^2\rangle^3$ has to be known for calculation of Z'_s. This ratio is invariant when the mEPSC amplitude distribution expands or shrinks, as is expected for uniform desensitization of receptors.

B.2.3. From kurtosis (fourth cumulant) and skewness

$$\langle\xi\rangle = \left(\frac{\lambda'^4_3}{\lambda'^3_4}\right)Z'_4 \tag{B.5}$$

$$Z'_4 = \frac{\langle h^4\rangle^3}{\langle h^3\rangle^4}\frac{I'^3_4}{I'^4_3} \tag{B.6}$$

This calculation is independent of background current, background variance, and offset current. It requires only the knowledge of $\langle h^4\rangle^3/\langle h^3\rangle^4$.

B.2.4. From kurtosis and skewness, when mEPSC amplitude is known

$$\langle\xi\rangle = \frac{\lambda'^2_3}{\lambda'_4}\frac{H'_s}{H'_4}\frac{1}{\langle h^2\rangle I_2} \tag{B.7}$$

This calculation uses lower powers of λ'_3 and λ'_4, and therefore is less noisy. When mEPSC amplitude is known, it is also straightforward to calculate the rate from skew alone, according to

$$\xi = \frac{\lambda'_3}{\langle h^3\rangle I'_3} \tag{B.7a}$$

B.3. Calculating the mean mEPSC amplitude

B.3.1. From variance and deconvolution, applying corrections for background variance, channel variance, and offset current

It is assumed that a deconvolution was performed, using the assumed mEPSC amplitude h_0 and resulting in a deconvolution rate ξ_0 (usually a time dependent quantity!). Then the actual rate can be calculated as $\xi = \xi_0 h_0/\langle h\rangle$. Insertion into Eq. (B.1) yields,

$$\langle h\rangle = (\lambda'_2 - \lambda'_{2,o} - i'(I_p - I_{p,o}))\frac{H'_v}{(\xi_0 h_0)} \tag{B.8}$$

and

$$\langle\xi\rangle = \frac{(\xi_o h_o)^2}{(\lambda'_2 - \lambda'_{2,o} - i'(I_p - I_{p,o}))H'_v} \tag{B.8a}$$

B.3.2. From skew and variance, applying corrections for background variance, channel variance, and offset current

$$\langle h\rangle = \frac{\lambda'_3}{(\lambda'_2 - \lambda'_{2,o} - i'(I_p - I_{p,o}))}H'_s \tag{B.9}$$

$$H'_s = \frac{\langle h^2\rangle\langle h\rangle}{\langle h^3\rangle}\frac{I'_2}{I'_3} \tag{B.10}$$

B.3.3. From kurtosis (fourth moment) and skewness

$$\langle h \rangle = \frac{\lambda_4'}{\lambda_3'} H_4' \tag{B.11}$$

$$H_4' = \frac{\langle h^3 \rangle \langle h \rangle}{\langle h^4 \rangle} \frac{I_3'}{I_4'} \tag{B.12}$$

B.3.4. Calculating the variance contribution of mEPSCs (V_m') to total variance from skew and kurtosis

$$V_{\mathrm{m}}' = \xi \langle h^2 \rangle I_2 = \frac{\lambda_3'^2}{\lambda_4'} \frac{H_{\mathrm{s}}'}{H_4'} \tag{B.13}$$

This calculation does not require knowledge about channel variance, nor background variance.

B.3.5. Calculating the variance contribution of channel fluctuations (V_c') from total variance, skew and kurtosis

$$V_{\mathrm{c}}' = \lambda_2' - \lambda_{2,\mathrm{o}}' - \frac{\lambda_3'^2}{\lambda_4'} \frac{H_{\mathrm{s}}}{H_4} \tag{B.14}$$

B.3.6. Calculating the apparent single channel current i' as the ratio between V_c' and $(I_p - I_{p,o})$

$$i' = \frac{\lambda_2' - \lambda_{2,\mathrm{o}}'}{(I_{\mathrm{p}} - I_{\mathrm{p,o}})} \left(1 - \frac{1}{\lambda_2' - \lambda_{2,\mathrm{o}}'} \frac{\lambda_3'^2}{\lambda_4'} \frac{H_{\mathrm{s}}'}{H_4'} \right). \tag{B.15}$$

References

Anderson C, Stevens C. Voltage clamp analysis of acetylcholine produced end-plate current fluctuations at frog neuromuscular junction. J Physiol 1973;235:655–91.

Aumann Y, Parnas H. Evaluation of the time course of neurotransmitter release from the measured PSC and MPSC. Bull Math Biol 1991;53:537–55.

Barbour B, Häusser M. Intersynaptic diffusion of neurotransmitter. Trends Neurosci 1997;20:377–84.

Barbour B, Keller BU, Llano I, Marty A. Prolonged presence of glutamate during excitatory synaptic transmission to cerebellar Purkinje cells. Neuron 1994;12:1331–43.

Bevington PR. Data reduction and error analysis for the physical sciences. San Francisco: McGraw-Hill; 1969. 336 pp.

Borges S, Gleason E, Turelli M, Wilson M. The kinetics of quantal transmitter release from retinal amacrine cells. Proc Natl Acad Sci USA 1995;92:6896–900.

Borst JGG, Sakmann B. Calcium influx and transmitter release in a fast CNS synapse. Nature 1996;383:431–4.

Carter AG, Regehr WG. Prolonged synaptic currents and glutamate spillover at the parallel fiber to stellate synapse. J Neurosci 2000;20: 4423–34.

Clements JD. Variance–mean analysis: a simple and reliable approach for investigating synaptic transmission and modulation. J Neurosci Methods 2003;130:115–25.

Colquhoun D, Hawkes AG. On the stochastic properties of single ion channels. Proc R Soc Lond B: Biol Sci 1981;211:205–35.

Del Castillo J, Katz B. Statistical factors involved in neurotransmitter facilitation and depression. J Physiol 1954;124:574–85.

Diamond JS, Jahr CE. Asynchronous release of synaptic vesicles determines the time course of AMPA receptor-mediated EPSC. Neuron 1995;15:1097–107.

Faber DS, Korn H. Synergism at central synapses due to lateral diffusion of transmitter. PNAS 1988;85:8708–12.

Faber DS, Young WS, Legendre P, Korn H. Intrinsic quantal variability due to stochastic properties of receptor–transmitter interactions. Science 1992;258:1494–8.

Fesce R. Stochastic approaches to the study of synaptic function. Prog Neurobiol 1990;35:85–133.

Fesce R, Segal JR, Hurlbut WP. Fluctuation analysis of nonideal shot noise. Application to the neuromuscular junction. J Gen Physiol 1986;88:25–57.

Hartzell HC, Kuffler SW, Yoshikami D. Post-synaptic potentiation: interaction between quanta of acetylcholine at the skeletal neuromuscular synapse. J Physiol 1975;251:427–63.

Heinemann SH, Sigworth FJ. Open channel noise. VI. Analysis of amplitude histograms to determine rapid kinetic parameters. Biophys J 1991;60:577–87.

Joshi I, Wang LY. Developmental profiles of glutamate receptors and synaptic transmission at a single synapse in the mouse auditory brainstem. J Physiol 2002;540:861–73.

Katz B. The release of neural transmitter substances. Liverpool: Liverpool University Press; 1969.

Katz B, Miledi R. The statistical nature of the acetylcholine potential and its molecular components. J Physiol 1972;224:665–700.

Kendall MG. The advanced theory of statistics. London: Charles Griffin & Company; 1947. p. 49–74.

Kinney GA, Overstreet LS, Slater NT. Prolonged physiological entrapment of glutamate in the synaptic cleft of cerebellar unipolar brush cells. J Neurophysiol 1997;78:1320–33.

Lu T, Trussell LO. Inhibitory transmission mediated by asynchronous transmitter release. Neuron 2000;26:683–94.

Mennerick S, Zorumski CF. Presynaptic influence on the time course of fast excitatory synaptic currents in cultured hippocampal cells. J Neurosci 1995;15:3178–92.

Meyer A, Neher E, Schneggenburger R. Estimation of quantal size and number of functional active zones at the Calyx of Held synapse by non-stationary EPSC variance analysis. J Neurosci 2001;21:7889–900.

Neher E, Sakaba T. Combining deconvolution and noise analysis for the estimation of transmitter release rates at the Calyx of Held. J Neurosci 2001a;21:444–61.

Neher E, Sakaba T. Estimating transmitter release rates from postsynaptic current fluctuations. J Neurosci 2001b;21:9638–54.

Neher E, Stevens CF. Conductance fluctuations and ionic pores in membranes. Annu Rev Biophys Bioeng 1977;6:345–81.

Oleskevich S, Clements J, Walmsley B. Release probability modulates short-term plasticity at a giant terminal. J Physiol (Lond) 2000;524:512–23.

Otis TS, Wu YC, Trussell LO. Delayed clearance of transmitter and the role of glutamate transporters at synapses with multiple release sites. J Neurosci 1996;16:1634–44.

Quastel DM. The binomial model in fluctuation analysis of quantal transmitter release. Biophys J 1997;72:728–53.

Reid CA, Clements JD. Postsynaptic expression of long-term potentiation in the dentate gyrus demonstrated by variance–mean analysis. J Physiol 1999;518:121–30.

Rice SO. Mathematical analysis of random noise. Bell Telephone Syst J 1944;23:282–332.

Sakaba T, Neher E. Quantitative relationship between transmitter release and calcium current at the Calyx of Held synapse. J Neurosci 2001;21:462–76.

Scheuss V, Neher E. Estimating synaptic parameters from mean, variance and covariance in trains of synaptic responses. Biophys J 2001;81:1970–89.

Scheuss V, Schneggenburger R, Neher E. Separation of presynaptic and postsynaptic contributions to depression by covariance analysis of suc-

cessive EPSCs at the Calyx of Held synapse. J Neurosci 2002;22:728–39.

Schneggenburger R, Neher E. Intracellular calcium dependence of transmitter release rates at a fast central synapse. Nature 2000;406: 889–93.

Segal JR, Ceccarelli B, Fesce R, Hurlbut WP. Miniature endplate potential frequency and amplitude determined by an extension of Campbell's theorem. Biophys J 1985;47:183–202.

Sigworth F. The variance of sodium current fluctuations at the node of Ranvier. J Physiol 1980;307:97–129.

Silver RA, Momiyama A, Cull-Candy SG. Locus of frequency-dependent depression identified with multiple-probability fluctuation analysis at rat climbing fibre-Purkinje cell synapses. J Physiol (Lond) 1998;510: 881–902.

Spiegel MR. Theory and problems of probability and statistics. Schaum's outline series. New York: McGraw-Hill; 1975. 372 pp.

Taschenberger H, Leao RM, Rowland KC, Spirou GA, von Gersdorff H. Optimizing synaptic architecture and efficiency for high-frequency transmission. Neuron 2002;36:1127–43.

Trussell LO, Zhang S, Raman IM. Desensitization of AMPA receptors upon multiquantal neurotransmitter release. Neuron 1993;10:1185–96.

Van der Kloot WJ. Estimating the timing of quantal releases during end-plate currents at the frog neuromuscular junction. J Physiol 1988a;402: 595–603.

Van der Kloot WJ. The kinetics of quantal releases during end-plate currents at the frog neuromuscular junction. J Physiol 1988b;402:605–26.

Vere-Jones D. Simple stochastic models for the release of quanta of transmitter from a nerve terminal. Aust J Stat 1966;8:53–63.

Vorobieva ON, Hackett JT, Worden MK, Bykhovskaia MK. Evaluation of quantal neurosecretion from evoked and miniature postsynaptic responses by deconvolution method. J Neurosci Methods 1999;92: 91–9.